e-PRESERVATIONScience

e-PS, 2014, 11, 15-21
ISSN: 1581-9280 web edition
ISSN: 1854-3928 print edition

e-Preservation Science (e-PS)

is published by Morana RTD d.o.o.
www.Morana-rtd.com

Copyright M O R A N A RTD d.o.o.

SCIENTIFIC PAPER

AN INVESTIGATION OF WEIGHTED AND DEGRADED SILKS BY COMPLEMENTARY MICROSCOPY TECHNIQUES

Paul Garside[1]*, Graham A. Mills[2], James R. Smith[2], Paul Wyeth[3]

1. The British Library, 96 Euston Road, London NW1 2DB, UK.

2. School of Pharmacy and Biomedical Sciences, University of Portsmouth, St Michael's Building, White Swan Road, Portsmouth, Portsmouth PO1 2DT, UK.

3. Centre for Textile Conservation and Technical Art History, Robertson Building University of Glasgow, Glasgow G11 6AQ, UK.

corresponding author:
paul.garside@bl.uk

Abstract

A number of silk samples, comprising historic materials and modern surrogates, were examined by light, electron and atomic force microscopy, to determine the extent to which such assessments would allow the nature and condition of the materials to be determined. The integrity of these materials had previously been investigated using mechanical testing. Signs of deterioration, such as surface debris, defibrillation and micro-fractures were readily observed. However, when these features were compared to the overall deterioration of the samples (as assessed by tensile strength), it became apparent that obvious surface damage did not necessarily correspond to overall levels of deterioration and that many samples which appeared in good condition under microscopic examination were in fact heavily degraded. This will have implications for the assessment of these materials, as microscopy will not necessarily reveal how well an artefact may stand up to the rigours of handling, display and conservation.

1 Introduction

Silk is a valuable fibre found in many artefacts of historic and cultural significance. Therefore it is necessary to have a good understanding of the properties and behaviour of this material in order to effectively conserve these aspects of our cultural heritage for future generations.

The fibre is produced by silkworms, the larval stage of the silk moth, to form a protective cocoon; the majority of commercially produced silk comes from the domesticated moth, *Bombyx mori*.[1-10] In its native form, the material consists of a pair of filaments with roughly triangular cross-section ('brins'), formed of the protein fibroin, cemented together by a second protein sericin. The brins may be up to a kilometre or more in length, and are highly crystalline, being predominantly composed of three amino acids alanine, glycine, and serine, in the hexapeptide motif -Gly-Ala-Gly-Ala-Gly-Ser-, which allows anti-parallel β-sheet secondary structures to form. The remainder of the protein forms an amorphous matrix in which the β-crystallites, arranged in a hierarchy of fibrillar elements, are embedded. This extensive crystallinity gives silk (fibroin) filaments their characteristic strength, chemical resistance, lustre and low extensibility.[2-4,6,8] Sericin, on the other hand, is largely formed of amino acids with bulky, polar side-chains, which prevent long-range ordering of the polymer, and impart a solubility (for example, in hot alkaline water) which allows sericin to be removed from fibroin with minimal damage to the latter; this process is applied to most commercial silks, and is known as 'degumming'.[2-4,10]

In addition to the inherent properties of the fibre, it is also necessary to consider the way in which fibres and fabrics may have been treated during their production. For silk, there are two particularly important historic processing methods - weighting and bleaching.[1,11,12] Weighting (using organic agents such as gums, sugars and protein glues) was originally employed as a means of replacing the mass lost during degumming, as the material was sold on the basis of weight. Subsequently, this became an accepted method of

received: 03/10/2013

accepted: 21/02/2014

key words:
silk, textiles, conservation, microscopy, scanning electron microscopy, atomic force microscopy

imparting a particular texture and drape.[1,11] By the late 18th century, these organic materials had started to be replaced by metal salts which form insoluble complexes within the fibre. These materials have a better washfastness; however, they are also implicated in the long-term deterioration of the material. During the same period (late 18th to 20th centuries), the bleaching of silk was commonly achieved by 'sulphur stoving', a process which involved exposing the material to the fumes of burning sulphur (sulphur dioxide) which then formed sulphurous acid, the active bleaching agent, on contact with moisture in the fibres.[12] This process is also deleterious to the stability of silk. Both weighting and sulphur stoving were particular to the European silk industry, which helps to explain the generally better condition of many contemporaneous Asian silks. Sulphur compounds may also be found on silk as a result of the application of sulphuric acid to give the material a characteristic rustle and texture ('scroop'), and treatment with sulphuric acid was also employed in the production of silk crêpe.[13,14]

In conservation, microscopy is widely used to identify fibres and assess their condition, and may be used in conjunction with other approaches, such as the traditional burn or dissolution tests or more advanced methods such as vibrational spectroscopy.[14] Light microscopy (LM) is widely used as a simple, rapid and ready available technique to identify fibres and, if possible, to assess their condition and the possible presence of processing treatments or other modification. Identification can be achieved thanks to the characteristic morphologies of the different natural fibre types, and may be assisted by the use of polarised light, specific dyes or solvents.[14-16] The presence of applied treatments, such as glazes, adhesives and pigment particles, can also often be recognised, providing greater information about the composition of the artefact. Damage to the fibre may also be seen, usually manifesting as surface debris, fracturing and defibrillation,[17-21] and this type of observation is often important when considering appropriate conservation measures where the condition of the material will influence the degree of intervention required and the delicacy with which it must be carried out. As a result, it is necessary to be confident that microscopy will reliably allow materials to be characterised in this way. We therefore used three microscopic techniques to assess a variety of silk samples, including specimens taken from historic textiles and surrogates prepared using historically accurate methods and subjected to accelerated ageing.[22,23] The methods employed were chosen to reveal complementary information about the materials: LM, in transmission mode; scanning electron microscopy (SEM), using secondary electron imaging; and atomic force microscopy (AFM). Both LM and SEM are used widely in conservation, but AFM is a relatively novel technique in the field.

AFM is a high-resolution microscopic technique that does not require specimens to be metal-coated or stained and does not use high energy electron beams or ultra high vacuum conditions that can cause sample damage.[24] AFM has been used to image silk fibroin from *Bombyx mori* cast onto mica, gold-coated quartz crystals and polystyrene,[25-27] the morphology and microstructure of *B. mori* silk/poly(ethylene oxide) (PEO) fibres[28] and the interior surfaces of dragline silk of the spider *Nephila clavipes*.[29,30] Surfaces of stretched and unstretched silk fibres from the spider *Latrodectus hesperus* (black widow) have also been imaged using AFM. Here two types of fibre, in terms of thickness and fibril orientation with respect to the thread axis, were identified.[31] The wicking behaviour of silk fabrics treated with fluorocarbon coatings has been investigated using AFM, where increased surface roughness was observed after exposure of the treated silk to UV light (λ = 172 nm, 50 mW cm^{-2}, 10 min).[32] The increased roughness was attributed to erosion caused by oxygen radicals. AFM has also been used to measure stretching forces of silk fibres.[33]

The condition of the fibres was assessed using mechanical testing to derive tensile strength. This was chosen as an appropriate marker for deterioration as all forms of damage, whether chemical, photo-induced or physical, will ultimately impair the integrity of the fibre and thus lead to a loss of strength, allowing this value to be used as a non-pathway specific indicator.

2 Method

Plain weave, undyed habutae silk samples were weighted and processed by a variety of historical methods; some were then subjected to artificial ageing. The original silk fabric was woven from reeled (full length) brins, with approximately 46 warp yarns cm^{-1} by 50 weft yarns cm^{-1} (with 20 $\pm$ 3 silk fibres per yarn), and a mass of 0.0036 g cm^{-2}; the silk was degummed. The following weighting regimes were employed: 'pink' tin (tin(IV) chloride), with up to three applications of the weighting agents; 'dynamite' tin (tin(IV) chloride, aluminium sulphate and sodium silicate), with up to two applications; and iron (iron(II) sulphate) with up to three applications (general methods are given in Carboni[1]; the specific applications used in this experiment, as well as the artificial ageing methods, are given in Garside[22]). In addition, a set of samples were bleached by 'sulphur stoving' (exposure to fumes of burning sulphur, yielding sulphurous acid) some of which were then also weighted using the 'pink' tin method, with one and three applications of the weighting agent.[12,22] The changes in mass (with respect to the original, degummed mass) are presented in Table 1. The number of applications of a particular weighting regime is indicated by the use of '(×*n*)'; for example, 'Dynamite (×2)' refers to the sample weighted twice by the dynamite method. A number of historic silks were also used as reference specimens. These samples were then assessed using LM, SEM and AFM.

Samples for transmitted LM were permanently mounted on glass slides using DPX resin mounting medium (Agar Scientific, UK). They were examined using a Leica DMR-XE microscope in transmitted light mode. Digital micrographs were recorded using a MediaCybernetics QICam 5.0 RTV (Marlow, UK), and were then interrogated using ImagePro Plus software to measure fibre dimensions (specifically fibre width).

Samples for SEM were mounted on aluminium stubs using conductive adhesive pads, and gold coated using a sputter coater (*ca.* 20 nm thickness). These specimens were then examined using a Philips XL30 ESEM (FEI, Eindhoven, The Netherlands), in secondary electron imaging mode.

For AFM imaging, fibres were mounted on magnetic nickel discs using conductive adhesive tape and placed on the AFM scanner. A MultiMode/NanoScope IV Scanning Probe Microscope (Digital Instruments, Santa Barbara, CA, USA; Bruker software Version 6.11r1) was used and operated in air (temp = 23 °C, relative humidity = 30 %). Topography images (n = 3–5, different fibres) were obtained in TappingMode® (scan size = 2 µm × 2 µm, 500 × 500 pixels, scan rate = 1 Hz) using Si cantilevers with integrated tips (thickness = 3.5–4.5 µm, length = 115–135 µm, width = 30–40 µm, resonant frequency = 200–400 kHz, spring constant (k) = 20–80 N m^{-1}, tip radius of curvature < 10 nm; Model: RTESP, Bruker Instruments, France). Surface roughness (R_a) measurements were single line transects (length 1.5 µm, total lines per image = 25, drawn across every acquired image, which were first-order levelled using a digital levelling algorithm; Bruker Image Analysis software V 7.10). R_a is obtained from the modulus of height deviations (z_i) from the mean height ($\bar{z}$) from the horizontal transect (n = 384, *i.e.*, 1.5 µm/2 µm × 512 pixels; Equation 1).[34]

$$R_a = \frac{1}{n}\sum_{i=n}^{n} \left| z_i - \bar{z} \right| \qquad \text{(Equation 1)}$$

Statistical analyses were performed using a one-way ANOVA and a *post-hoc* Tukey-Kramer test.[35]

Mechanical testing was employed to assess the integrity of the fibres after processing and ageing; tensile strength was taken as a non-specific marker of degradation, with a loss in strength indicating deterioration regardless of the precise mechanism of damage. Samples with a width of 10 mm and gauge length of 50 mm were extended at a rate of 10 mm min^{-1}, to breaking point, using an Instron 5544 rig and Bluehill software (High Wycombe, UK); extension was applied in the warp direction. Ten replicates were assessed per sample type, from which averages and standard deviations were calculated.

3 Results and Discussion

3.1 Light Microscopy

Typical light micrographs for the various treated and aged samples are presented in Figure 1. The average fibre widths after each treatment regime are given in Table 1 (the average in each case being calculated from single measurements from 50 separate fibres). As can be seen, both forms of tin weighting ('pink' and 'dynamite') lead to a significant increase in the diameter of the fibre, and regardless of the weighting regime there is a broad relationship between the mass gain and the increase in diameter of the fibre (Figure 2). In the more heavily weighted fibres (particularly the dynamite weighted silk) a granularity can also be observed as speckling (Figure 1).

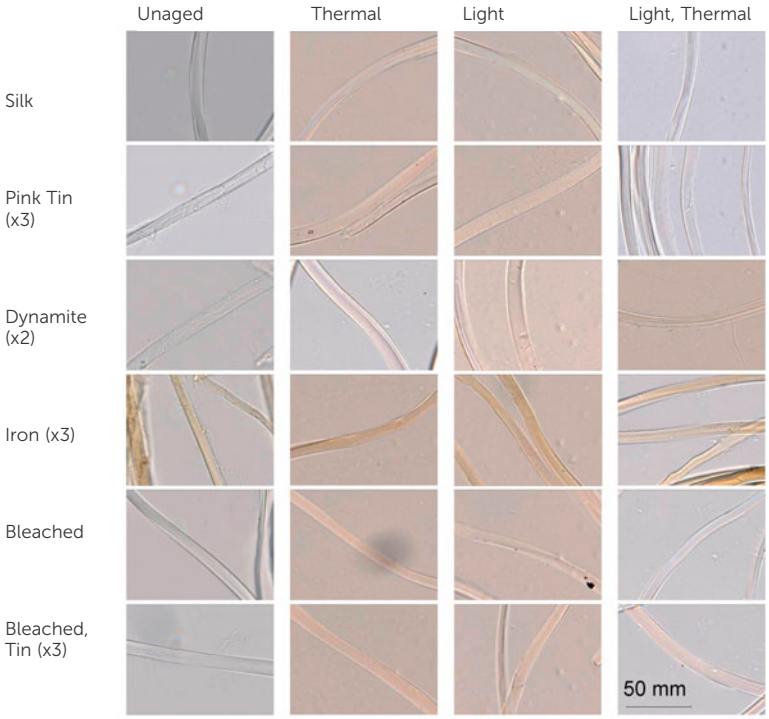

Figure 1: Typical light micrographs of weighted and aged silk fibres.

Sample	Mass Gain / %	Average Diameter / µm
Silk	0.0 (0.0)	10.9 (1.1)
Tin (×1)	15.2 (2.4)	11.8 (1.1)
Tin (×2)	33.3 (1.2)	12.7 (0.9)
Tin (×3)	53.7 (1.1)	12.6 (1.3)
Dynamite (×1)	48.8 (0.5)	12.0 (1.0)
Dynamite (×2)	99.0 (0.4)	13.9 (1.2)
Iron (×1)	6.3 (1.0)	10.8 (0.9)
Iron (×2)	11.9 (0.8)	10.8 (1.1)
Iron (×3)	17.3 (1.1)	11.1 (0.9)
Bleached	3.6 (0.7)	10.6 (0.8)
Bleached, Tin (×1)	17.2 (0.8)	12.6 (1.2)
Bleached, Tin (×2)	56.0 (2.7)	12.7 (1.0)

Table 1: Average diameters of silk samples, n = 50 (standard deviations are given in parentheses).

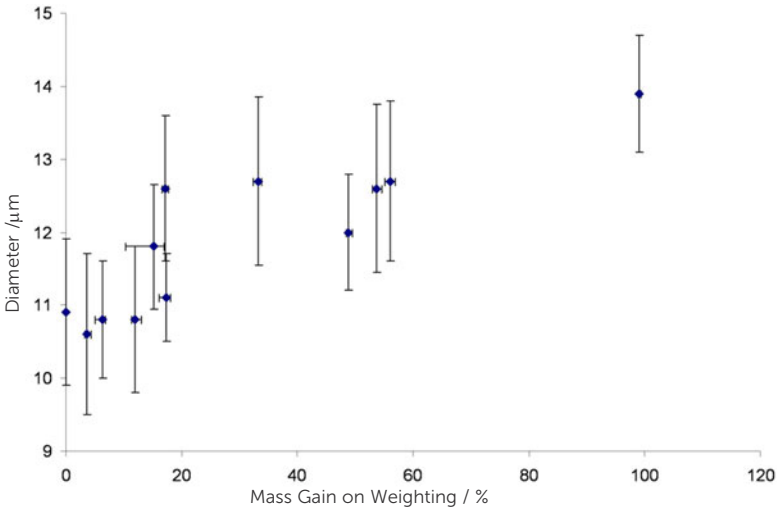

Figure 2: Variation of mass gain of weighting with average fibre diameter.

The light micrographs also demonstrate that the weighting processes appear to cause surface damage to the fibres, particularly in the form of defibrillation which can be observed as 'whiskers' of material detaching from the bulk fibre (Figure 1). However, if the mechanical data is considered (Table 2), it appears that this damage is superficial, as at this stage it is not accompanied by a significant loss in physical strength. After ageing (see Method; details given in Garside[22]), greater evidence of surface deterioration can be seen with more substantial defibrillation and deformation of the fibres themselves - many lose their generally uniform morphology, and may show evidence of significant losses of material.

The lack of specific surface detail available through light microscopy (due both to the transparency of the fibres and the small scale of the relevant features) means that it is difficult to assess the condition of these materials more accurately. However, it can be seen that in general there is more apparent damage to the thermally aged specimens than those that have been light aged, that the untreated silk and the bleached materials show less apparent damage through ageing than the weighted samples, and that of these latter fibres, those subject to iron weighting degrade more readily. To some extent this agrees with the assessment of deterioration through the measurement of tensile strength, but there are notable discrepancies, particularly that although light ageing can cause a catastrophic loss in strength, it does not appear to be accompanied by extensive observable damage.

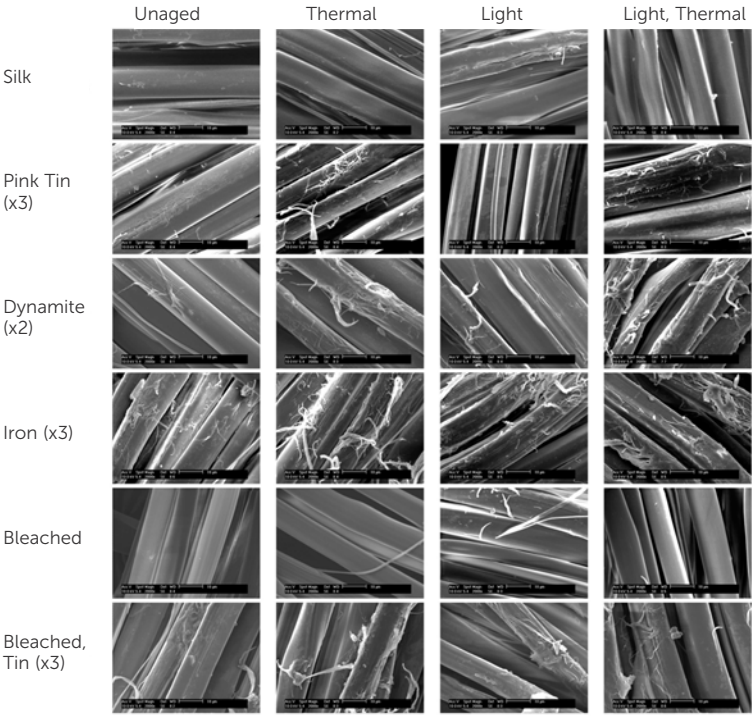

Figure 3: Typical SEM images of weighted and aged silk fibres.

Sample	Tensile Strength / N				
	Un-aged	Thermal ageing 2 Weeks	Thermal ageing 4 Weeks	Light Ageing	Combined Light and Thermal Ageing
Silk	71.2 (1.2)	59.8 (1.3)	55.3 (3.2)	29.4 (4.8)	12.2 (3.1)
Tin (x1)	65.4 (0.9)	57.3 (1.9)	51.8 (2.0)	9.7 (1.0)	6.2 (0.7)
Tin (x2)	63.2 (0.6)	58.5 (1.4)	55.1 (2.7)	—	—
Tin (x3)	64.1 (1.8)	57.1 (0.7)	54.1 (0.5)	9.2 (1.7)	3.2 (0.4)
Dynamite (x1)	66.3 (2.2)	57.1 (1.4)	55.6 (3.0)	—	—
Dynamite (x2)	59.7 (2.0)	49.2 (4.6)	35.7 (5.6)	17.5 (6.4)	6.9 (1.0)
Iron (x1)	58.3 (1.2)	60.1 (2.2)	56.8 (0.7)	—	—
Iron (x2)	45.5 (1.7)	—	—	—	—
Iron (x3)	41.7 (2.5)	18.4 (2.0)	6.4 (2.6)	7.4 (1.0)	3.8 (0.6)
Bleached	58.0 (1.8)	45.4 (4.6)	31.7 (7.2)	19.4 (4.8)	5.4 (0.5)
Bleached, Tin (x1)	61.0 (1.0)	51.6 (3.1)	45.0 (1.2)	—	—
Bleached, Tin (x3)	63.4 (5.0)	59.8 (1.2)	56.6 (0.8)	11.2 (1.0)	7.9 (2.8)

Table 2: Tensile strengths of treated and aged silk samples (standard deviations are given in parentheses).

3.2 Scanning Electron Microscopy

The SEM micrographs largely confirm the phenomena observed using LM, and allow more detailed inferences to be drawn about the effects of ageing (Figure 3).

The surface damage (defibrillation) caused by weighting is immediately apparent, and is not observed in either the untreated or the bleached silks. Thermal ageing exacerbates this, causing more damage to the fibrillar structure, microfracturing and loss of material. This is not, however, observed to the same extent with the light aged samples (except for the iron weighted specimens); again, the apparent damage to the non-weighted silks is much less significant.

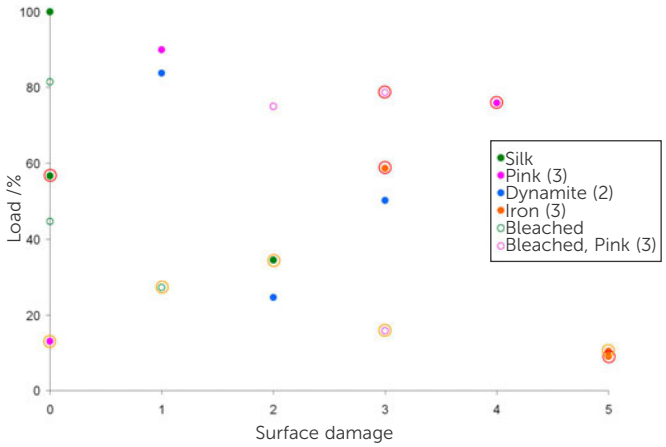

Figure 4: Plot of the surface damage observed using SEM (subjectively graded 0–5) versus the maximum breaking load of the samples (relative to un-aged silk, expressed as a percentage). Data for un-aged, and sunlight equivalent (gold ring) and thermal and humidity (red ring) aged specimens are included.

When these observed features are compared to the mechanical properties of the fibres, again it can be seen that apparent damage does not necessarily correspond to losses in tensile strength. Thermal ageing results in much more significant surface damage than light ageing, but the former does not compromise the bulk integrity of the fibre to the same extent as the latter. Bleaching has a very deleterious effect on the stability of the material, especially under thermal ageing conditions, but causes little observable surface damage.

This conclusion is emphasised in Figure 4, which shows a plot of the apparent degree of surface damage (subjectively assessed from the SEM images, on a coarse scale 0–5 based on the degree of increased surface pitting and fracturing, defibrillation and accumulation of surface debris when compared to undamaged silk) versus the maximum load on of the samples (relative to un-aged silk). Two broad trends are discernible, with the un-aged and thermal and humidity aged weighted silks exhibiting behaviour distinct from the other specimens.

3.3 Atomic Force Microscopy

AFM revealed the outer surface of silk fibres taken from the original habutae silk fabric to have striations in parallel to the long axis of each fibre (Figure 5). These features were found to have variable widths of 86 ± 22 nm (Figure 6), which are in good agreement to widths of fibrils from native silk observed elsewhere (90–170 nm).[36] Fibrillar elements are known to be embedded within an amorphous matrix that aligns along the fibre axis during extrusion.[1-9]

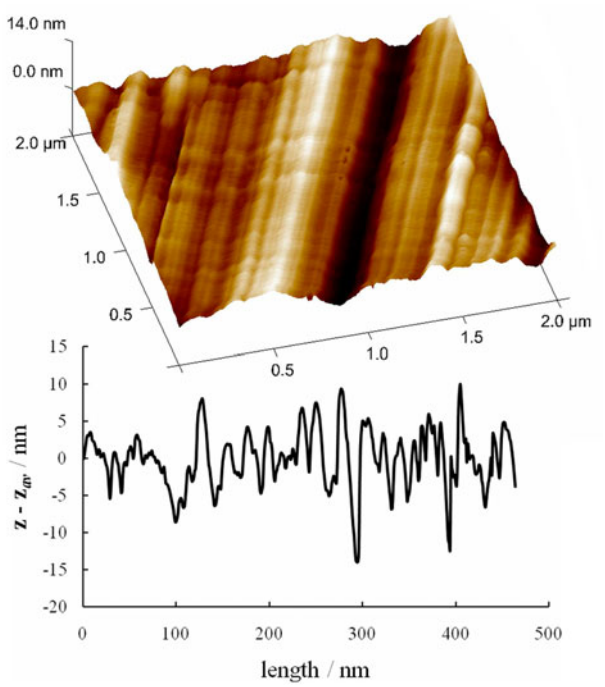

Figure 5: (a) A typical AFM image of the outer surface of an untreated silk fibre; (b) a line profile across the striations perpendicular to the long axis of the fibre showing dimensions of fibrils.

Tin weighting (×1) was found to slightly increase the width of the fibrils (98 ± 21 nm) and increase the R_a from 1.9 ± 0.7 nm (untreated) to 2.1 ± 0.8 nm ($p < 0.05$; Figure 6a; Table 3). This supports the LM observation that weighting leads to the swelling of the fibre, as the metal salts are absorbed within the amorphous interfibrillar matrix. The fibrils became less apparent with further tin weighting (×3), although surface deposits could be seen due to the increased presence of the additional material (Figure 6b); in this instance, the deposits did not significantly change R_a (2.4 ± 0.9 nm) from the tin (×1) sample (Table 3). Similar deposits were observed for silk fibres which had been light aged either with or without tin weighting (×3); Figures 6c and 6d, respectively, although a marginally, but statistically, rougher surface was apparent for the former surface (R_a = 4.6 ± 2.9 nm and 4.4 ± 2.1 nm, respectively, $p < 0.05$; Table 3). Thermally aged non-weighted fibres were found to be less rough than light aged surfaces (R_a = 3.2 ± 1.5 nm and 4.6 ± 2.9 nm, respectively, $p < 0.05$; Table 3). For tin-weighted fibres (×3), thermal treatment was found to produce rougher surfaces than light ageing (R_a = 4.9 ± 2.5 nm and 4.4 ± 2.1 nm, respectively, $p < 0.05$; Table 3). This supports the LM and SEM observations that thermal ageing of tin-weighted fibres produces significantly more surface damage than light ageing, even though the latter generally causes greater damage to the bulk fibre, as indicated by a greater loss in tensile strength.

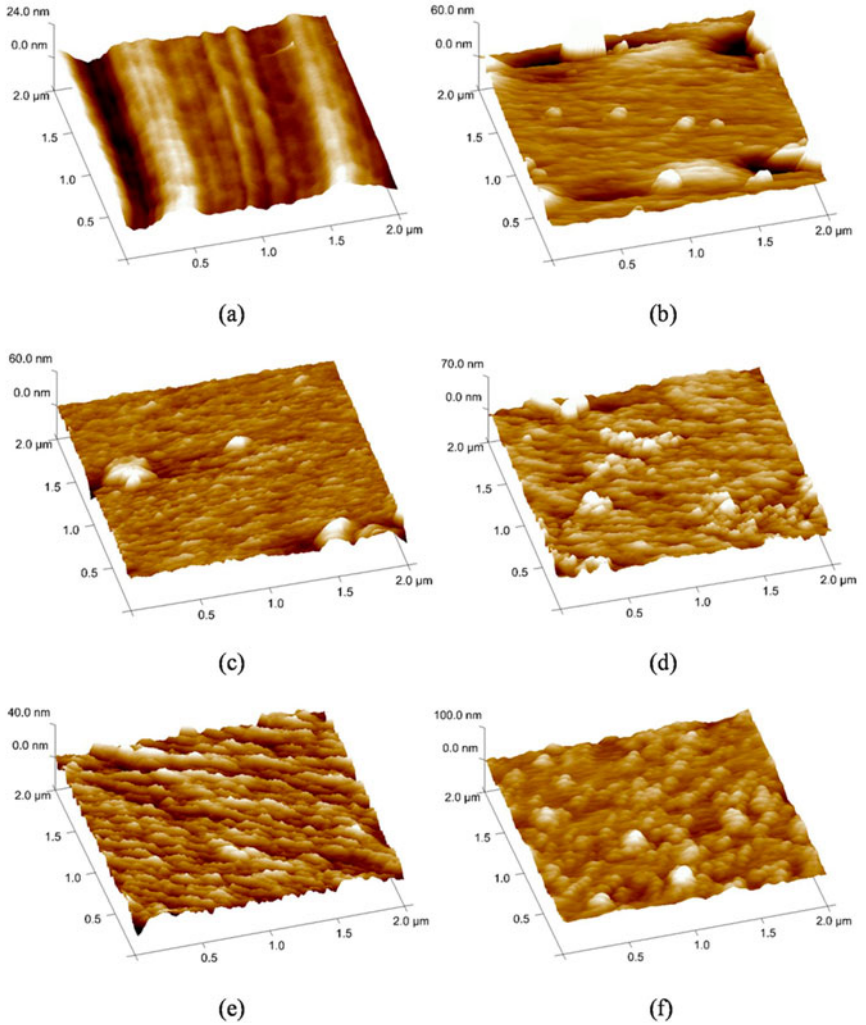

Figure 6: Typical AFM images of silk fibres subjected to various treatments: (a) tin (×1), (b) tin (×3), (c) light aged, (d) tin (×3) and light aged, (e) thermally aged, (f) tin (×3) and thermally aged.

Large standard deviations (SD) in R_a measurements were observed,

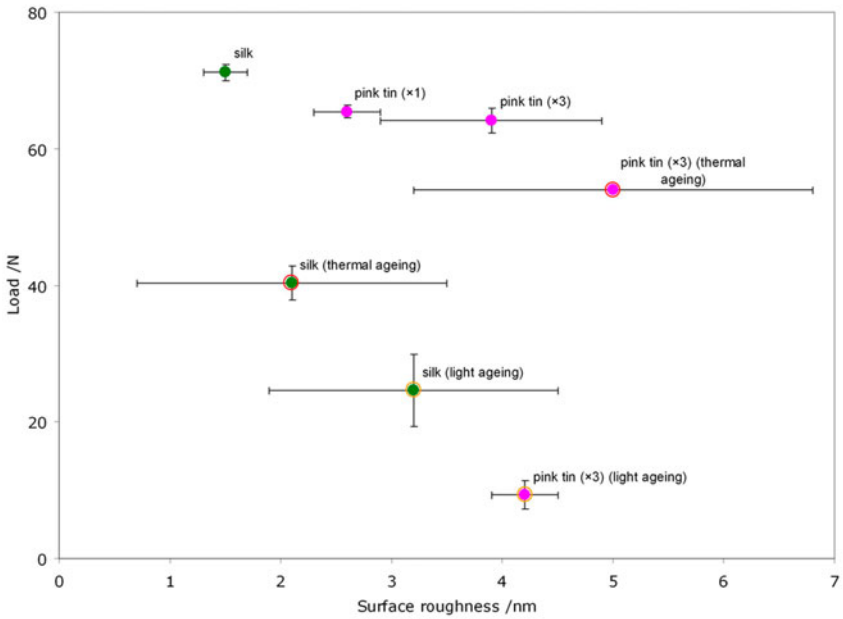

Figure 7: Variation of surface roughness (R_a; determined by AFM) with maximum loads for unaged, sunlight (l) and thermal and humidity (t + h) aged silks (unweighted and pink tin weighted). Standard deviations (SD) are indicated.

Treatment	Surface roughness, Ra / nm	SD / nm	N
Untreated	1.9	0.7	125
Light aged	4.6	2.9	75
Thermally aged	3.2	1.5	100
Tin (x1)	2.1	0.8	75
Tin (x3)	2.4	0.9	25
Tin (x3) light aged	4.4	2.1	75
Tin (x3) thermally aged	4.9	2.5	100

Table 3: Effect of silk treatment on surface roughness.

however, probably reflecting the heterogeneous effects of the various treatments of the silk fibres. For example, all treatments produced higher SD values than that for untreated silk (Table 3). Generally, harsher fibre treatments (as reflected by lower maximum tensile loads) tended to produce higher R_a SD values (Figure 7), again reflecting heterogeneity of the treatment. Moreover, a general inverse relationship between load and R_a was observed, suggesting that the latter parameter could provide a quantitative marker of condition (Figure 7).

4 Conclusion

The three forms of microscopy used in this study can be used to reveal useful information about silk fibres, including those subjected to historically common processing methods and subsequently aged. However, it is also apparent that microscopy has significant limitations for certain materials, and consequently may give misleading results if used to assess the degree of deterioration (in this study using tensile strength as a non-specific indicator) suffered by these specimens. This is significant as microscopy (particularly LM) is often used in conservation practice as a rapid and simple method of identifying fibres and gaining a better understanding of their condition.

Even relatively simple (and, in the context of conservation, readily available) LM can help to identify those materials which have been subjected to weighting, by subtle variations in dimension and by the presence of granular aggregates within the fibre, usually in combination with a change in texture when handled. Gross surface damage, particularly in the form of defibrillation and deformation, can be observed.

SEM, a technique which is relatively widely available in conservation, can give further information, with surface deposits apparently following weighting. Both defibrillation and surface fracturing, which is not readily observed by LM, can be seen, and fibrillar structures at the surface may be observed even before significant damage can be seen.

Although AFM is not routine in most conservation practices, it can be seen that it is an important method for probing the structure of materials and allowing a greater insight into their properties and behaviour. In this study, the ability to accurately measure fibril separation permitted a greater understanding of the swelling of the fibres with weighting previously observed using LM and SEM. The measurement of roughness, R_a, gives a quantitative measurement of surface irregularity, which is related to fibre damage through effects such as defibrillation and microfracturing; these have previously been observed in a qualitative manner with the other microscopic techniques. Figure 7 shows that R_a can be used as a semi-quantitative indicator of overall damage as a result. However, when microscopic features observed with all three techniques are compared to the tensile strengths of the materials, it can be seen that there are certain discrepancies between apparent damage and actual physical integrity. Therefore, microscopic examination of materials of this kind must be used with caution, as fibres which appear to have suffered extensive damage may in fact be in relatively good condition, with the degradation limited to the superficial surface layers, whereas samples which seem to be free from damage can instead have suffered a substantial loss of integrity due to internal damage which cannot be readily seen. Nonetheless, with an understanding of the limitations of each of the individual techniques, they may give valuable insights into the condition of historic silk fibres, and by applying them in a complementary fashion, much useful information can be obtained.

5 Acknowledgements

PG and PW would like to thank the AHRC who provided funding for their research whilst they were employed at the Textile Conservation Centre (University of Southampton), as well as Mary Brooks (Textile Conservation Centre), Sarah Howard (Hampshire County Council Museums and Archives Services, Winchester) and David Howell (Bodleian Library, Oxford) who acted as an advisory panel for the work; they would also like to thank their colleagues at

the Textile Conservation Centre for their support and advice.

6 References

1. P. Carboni, *Silk: Biology, Chemistry, Technology*, Chapman & Hall Ltd., London, UK, 1952.

2. W.G. Wolfgang, *Silk: Encyclopedia of Polymer Science and Technology*, **12**, John Wiley & Sons, Inc., New York, USA, 1970.

3. J.L. Merritt, *Silk: History, Cultivation and Processing*, Silk: Harpers Ferry Regional Textile Group (11th Symposium), 1992, 15-21.

4. M. Lewin, E.M. Pearce, Eds., *Handbook of Fiber Chemistry* (2nd Ed.), Marcel Dekker, Inc., New York, USA, 1998.

5. Z. Shao, F. Vollrath, Materials: surprising strength of silkworm silk, *Nature*, 2002, **418**, 741-751.

6. K. Mita, S. Ichimura, T.C. James, Highly repetitive structure and its organization of the silk fibroin gene, *J. Mol. Evol.*, 1994, **38**, 583-592.

7. A.U. Ude, R.A. Eshkoor, R. Zulkifili, A.K. Ariffin, A.W. Dzuraidah, C.H. Azhari, Bombyx mori silk fibre and its composite: A review of contemporary developments, *Mater. Design*, 2014, **57**, 298-305.

8. T. Gamo, T. Inokuchi, H. Laufer, Polypeptides of fibroin and sericin secreted from the different sections of the silk gland in Bombyx mori, *Insect Biochem.*, 1977, **7**, 285-295.

9. F. Lucas, K.M. Rudall, in: M. Florkin, K.M. Stotz (Eds.), *Comprehensive Biochemistry*, **26**, Elsevier Publishing Co., New York, 1968, pp. 475-558.

10. C. Fabiani, M. Pizzichini, M. Spadoni, G. Zeddita, Treatment of waste water from silk degumming process for protein recovery and water reuse, *Desal.*, 1996, **105**, 1- 9.

11. M. Hacke, Weighted silk: history, analysis and conservation, *Rev. Conservation*, 2008, **9**, 3-15.

12. S.H. Higgins, *Historic Bleaching*, Longs, Green & Co, London, UK, 1924.

13. E. Knecht, C. Rawson, R. Lowenthal, *A Manual of Dyeing: For the Use of Practical Dyers, Manufacturers, Students, and All Interested in the Art of Dyeing*, C. Griffin & J.B. Lippincott, London, UK, 1910.

14. A. Tímár-Balászy, D. Eastop, *Chemical Principles of Textile Conservation*, Butterworth-Heinemann, Oxford, UK, 1998.

15. Anon, *Identification of Textile Materials* (7th Ed.), The Textile Institute; Manchester, UK, 1985.

16. Anon, Fibre Identification Techniques; Textile Conservation Centre, 1998.

17. R.R. Bresee, G.E. Goodyear, *Fractography of Historic Silk Fibres*, in: H.L. Needles, S.H. Zeronian, Eds., *Historic Textile and Paper Materials (Advances in Chemistry, 212)*, American Chemical Society, Washington DC, USA, 1986, 95-110.

18. S.H. Zeronian, W. Alger, M.S. Ellison, S.M. Al-Khayatt, *Studying the Cause and Type of Fibre Damage in Textile Materials by Scanning Electron Microscopy*, in: H.L. Needles, S.H. Zeronian, Eds., *Historic Textile and Paper Materials (Advances in Chemistry, 212)*, American Chemical Society, Washington DC, USA, 1986, 77-94.

19. K. Mahall, *Quality Assessment of Textiles: Damage Detection by Microscopy* (2nd Ed.), Springer, New York, USA, 1993.

20. J.W.S. Hearle, B. Lomas, W.D. Cooke, *Atlas of Fibre Fracture and Damage to Textiles* (2nd Ed.), Woodhead Publishing Ltd., Oxford, UK, 1998.

21. M. Miraftab, Ed., *Fatigue Failure of Textile Fibres*, Woodhead Publishing Ltd., Oxford, UK, 2009.

22. P. Garside, P. Wyeth, X. Zhang, The Inherent Acidic Characteristics of Silk, Part II - Weighted Silks, *e-Preservation Science*, 2010, **7**, 126-131.

23. P. Garside, The Influence of Metal Weighting on the Stability of Silk, *Cultural Heritage Research Meets Practice*, University of Ljubljana, Ljubljana, 2008 (http://ec.europa.eu/research/environment/pdf/publications/fp7/cultural_heritage/chresp_preprint.pdf; retrieved 03/02/2014).

24. G. Binnig, C. Gerber, E. Stoll, T.R. Albrecht, C.F. Quate, Atomic resolution with atomic force microscope, *Surf. Sci. Lett.*, 1987, **A390**, 189-190.

25. S.I. Inoue, H. Tsuda, T. Tanaka, M. Kobayashi, Y. Magoshi, J. Magoshi, Nanostructure of natural fibrous protein: In vitro nanofabric formation of samia cynthia ricini silk fibroin by self-assembling, *Nanolett.*, 2003, **3**, 1329-1332.

26. E. Servoli, D. Maniglio, E. Motta, R. Predazzer, C. Migliaresi, Surface properties of silk fibroin films and their interaction with fibroblasts, *Macromol. Biosci.*, 2005, **5**, 1175-1183.

27. F. Junghans, M. Morawietz, U. Conrad, T. Scheibel, A. Heilmann, U. Spohn, Preparation and mechanical properties of layers made of recombinant spider silk proteins and silk from silkworm, *Appl. Phys. A*, 2006, **82**, 253-260.

28. M. Wang, H.-J. Jin, D.L. Kaplan, G.C. Rutledge, Mechanical properties of electrospun silk fibers, *Macromolecules*, 2004, **37**, 6856-6864.

29. D.V. Mahoney, D.L. Vezie, R.K. Eby, W.W. Adams, D. Kaplan, Aspects of the morphology of dragline silk of nephila clavipes, *ACS Symp. Series, Silk Polymers Mater.*, 1994, **544**, 196-210.

30. L.D. Miller, S. Putthanarat, R.K. Eby, W.W. Adams, Investigation of the nanofibrillar morphology in silk fibers by small angle x-ray scattering and atomic force microscopy, *Int. J. Biol. Macromol.*, 1999, **24**, 159-165.

31. S.A.C. Gould, K.T. Tran, J.C. Spagna, A.M.F. Moore, J.B. Shulman, Short and long range order of the morphology of silk from latrodectus hesperus (black widow) as characterized by atomic force microscopy, *Int. J. Biol. Macromol.*, 1999, **24**, 151-157.

32. S. Periyasamy, M.L. Gulrajani, D. Gupta, Preparation of a multifunctional mulberry silk fabric having hydrophobic and hydrophilic surfaces using VUV excimer lamp, *Surf. Coatings Technol.*, 2007, **201**, 7286-7291.

33. A. Schafer, T. Vehoff, A. Glisovic, T. Salditt, Spider silk softening by water uptake: an AFM study, *Eur. Biophys. J.*, 2008, **37**, 197-204.

34. J.R. Smith, S. Breakspear, S.A. Campbell, AFM in surface finishing. Part II. surface roughness, *Trans. IMF*, 2003, **81**, B55-B58.

35. C.P. Wheater, P.A. Cook, *Using Statistics to Understand the Environment* (1st Ed.), Taylor & Francis Ltd., London, UK, 2000.

36. S. Putthanarat, N. Stribeck, S.A. Fossey, R.K. Eby, W. Adams, Investigation of the nanofibrils of silk fibers, *Polymer*, 2000, **41**, 7735-7747.